

LA-UR-12-26114

Approved for public release; distribution is unlimited.

Title: Radiochemistry Results from IER-163 Comet Irradiation

Author(s): Sanchez, Rene G.
Attrep, Moses Jr.
Bounds, John Alan
Bredeweg, Todd Allen
Favorite, Jeffrey A.
Goda, Joetta M.
Hayes, David K.
Jackman, Kevin R.
Myers, William L.
Oldham, Warren J.
Rundberg, Robert S.
Schake, Ann R.

Intended for: Report



Disclaimer:

Los Alamos National Laboratory, an affirmative action/equal opportunity employer, is operated by the Los Alamos National Security, LLC for the National Nuclear Security Administration of the U.S. Department of Energy under contract DE-AC52-06NA25396. By approving this article, the publisher recognizes that the U.S. Government retains nonexclusive, royalty-free license to publish or reproduce the published form of this contribution, or to allow others to do so, for U.S. Government purposes. Los Alamos National Laboratory requests that the publisher identify this article as work performed under the auspices of the U.S. Department of Energy. Los Alamos National Laboratory strongly supports academic freedom and a researcher's right to publish; as an institution, however, the Laboratory does not endorse the viewpoint of a publication or guarantee its technical correctness.

Radiochemistry Results from the IER-163 COMET Irradiation

Rene G Sanchez¹, Moses Attrep Jr², John A Bounds¹, Todd A. Bredeweg², Jeffrey A Favorite³,

Joetta M Goda¹, David K Hayes¹, Kevin R. Jackman², William L Myers¹, Warren J Oldham²,

Robert S Rundberg², and Ann R Schake²,

¹ Los Alamos National Laboratory NEN-2: Advanced Nuclear Technology

² Los Alamos National Laboratory C-NR: Nuclear & Radiochemistry

³ Los Alamos National Laboratory X-CP7: Transport Applications

ABSTRACT

A critical experiment was performed on the Comet assembly to provide nuclear data in a non-thermal neutron spectrum and to re-establish experimental capability relevant to the Stockpile Stewardship and Technical Nuclear Forensic programs. Irradiation foils were placed at specific locations in the Zeus all or alloy critical experiment to obtain fission ratios and activation products. After the irradiation was completed and a cooling down period of time had elapsed, passive gamma ray measurements were performed on all the foils and several of the foils were packaged and shipped to Los Alamos National Laboratory (LANL) for further radiochemical analysis. The results from the Los Alamos National Laboratory's non-destructive and radiochemical analyses are presented. Monte Carlo simulations of the experiment are described and compared to the experimental results.

I. INTRODUCTION

The National Criticality Experiments Research Center (NCERC) at the Nevada National Security Site (NNSS) is home to four assemblies for use in conducting critical experiments. One of these assemblies is named Comet, which is a vertical-lift machine designed to support performance of experiments that are sub-critical or operate in the criticality regime at delayed critical and above but below prompt critical. Comet was the second of the four assemblies to be returned to service after the shutdown at TA-18 at the Los Alamos National Laboratory in 2004

In mid-2010, an Integral Experiment Request (IER-163) was submitted to the Nuclear Criticality Safety Program (NCSP) to support performance of a high-power irradiation of twelve foils using the Comet machine with a configuration from the Zeus series of critical experiments. The core for this configuration was fueled with cylindrical highly enriched uranium (HEU) metal plates surrounded by a large metallic copper reflector. The purpose of the experiment was to measure fission product activities, activation products (Ga, Ir, Au), fission ratios, and the amount of ²³⁷U created from ²³⁸U(n, 2n). Additionally, these irradiations were intended to help established the foundation for performing future irradiations such as

measuring reaction rates and fission-product chain yields. The results of the radiochemical destructive and non-destructive analyses of the six of the foils irradiated are presented here as well as the Monte Carlo simulations of these experiments. The intent of this report is to document the results and comparisons of the measurements and simulations to fulfill the reporting requirements for the fourth and final phase of the Critical Experiment Design (CED) process as established by the NCSP.

II. DESCRIPTION OF THE EXPERIMENT

II. A. Zeus Configuration

The Zeus series of experiments consist of a cylindrical core region that is surrounded on all sides by a metallic copper reflector. The core is divided into an upper portion and a lower portion. The upper portion rests on a thin, square stainless steel plate, called the diaphragm, which is supported by the inner corner copper reflectors. The bottom portion of the core sits on top of the bottom reflector. The bottom reflector, in turn, sits on the movable platen of the Comet vertical assembly machine as illustrated in Fig. 1. The lower portion of the core is held in position by a central, hollow aluminum alignment tube, the top of which is approximately 1/16-inch below the top unit on the movable platen. Two resistance temperature detectors (RTDs) are positioned inside the hollow aluminum alignment tube to measure the temperature increase during a high power run. The top, corner, and side reflectors rest on a stationary aluminum plate attached to the Comet machine.

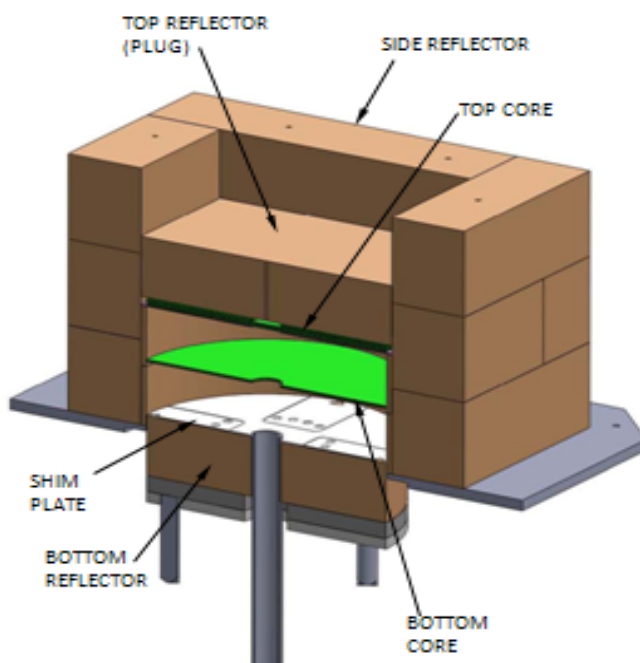


Figure 1. Final configuration showing the aluminum shims and the four trays where the irradiation foils were placed.

The experiment is assembled by raising the bottom portion of the assembly into a blind hole until it makes full contact with the steel diaphragm that supports the top portion of the core. For this experiment, the top portion of the core contained six HEU metal units. The bottom portion of the core

contained two HEU metal units plus a 1/8-in thick aluminum metal shim. The HEU metal units were constructed from the set of critical experiment parts known as the Jemima plates.¹ The aluminum metal shim was designed to have four aluminum metal trays with circular cavities machined where the irradiation foils are placed. A thin cover of aluminum metal foil was placed over the cavity openings where the foils resided to minimize the chance of cross contamination with the HEU metal unit that resided above. The trays were designed to slide out and away from the shim without having to remove units stacked above. The aluminum shim with its four aluminum trays containing irradiation foils was placed between the bottom copper reflector and the bottom HEU metal unit as shown in Fig. 1. Each HEU metal unit used in this experiment has two components, an inner disk and an outer ring. The inner disk in the bottom portion of the core and the top two inner disks in the top portion of the core have a 2.50-in diameter hole to accommodate the alignment tube. In contrast, the four remaining inner disks in the top portion of the core are solid pieces of HEU metal. All the HEU metal plates are approximately 0.118-in thick. The solid inner disks are 15-in in diameter. The inner disks with central holes are 15-in OD and 2.5-in ID. The outer rings are approximately 21-in OD and 15-in ID. Table I shows the weights and part numbers of each of the plates used in this critical experiment. The uranium metal plates are on average 93.22 wt% ²³⁵U, 1.11 wt% ²³⁴U, and 5.67 wt% ²³⁸U with an average mass density of 18.8 g/cc.

Table I. Description of uranium plates and their weights as loaded on the assembly.

Upper Portion of the Core					
Part Number	Description	Weight (g)	Part Number	Description	Weight (g)
B-2444-01	Outer Ring 21-in OD 15-in ID	6122.4	10464	Inner Disk 15-in OD 2.5-in ID	6259.2
B-2444-02	Outer Ring 21-in OD 15-in ID	6131.2	10475	Inner Disk 15-in OD 2.5-in ID	6235.8
B-2444-13	Outer Ring 21-in OD 15-in ID	6027.7	11017	Inner Disk 15-in Diameter Solid Plate	6516.8
B-2444-19	Outer Ring 21-in OD 15-in ID	6135.0	11149	Inner Disk 15-in Diameter Solid Plate	6405.4
B-2444-10	Outer Ring 21-in OD 15-in ID	6137.7	11147	Inner Disk 15-in Diameter Solid Plate	6523.6
B-2444-27	Outer Ring 21-in OD 15-in ID	6074.7	11150	Inner Disk 15-in Diameter Solid Plate	6429.2
Bottom Portion of the Core					
B-2444-33	Outer Ring 21-in OD 15-in ID	6158.6	10491	Inner Disk 15-in OD 2.5-in ID	6391.7
B-2444-29	Outer Ring 21-in OD 15-in ID	6131.7	10467	Inner Disk 15-in OD 2.5-in ID	6336.4
Aluminum Shim					
Total Uranium Mass 100,017.1 g					

II.B. Irradiations

The IER-163 irradiation was designed to have twelve foils irradiated in locations equidistant from the core axis. This required the insertion of a 1/8-in thick aluminum shim into the assembly where foils could be placed and easily recovered.² One of the irradiation sample trays loaded with foils is shown in Fig. 2.



Figure 2. **Samples loaded in Tray 3 prior to irradiation.**³

Six of these foils were measured, packaged, and shipped back to LANL for further analysis. Four of the foils were measured, packaged, and shipped to Pacific Northwest National Laboratory (PNNL) for further analysis. The final two foils were measured and remained at NCERC for future reuse. After the irradiation, the six LANL foils were measured in the NCERC counting room, packaged, and then shipped to TA-48 at LANL for further radiochemical analysis. Four of the foils were chemically dissolved and destructive analysis was performed on them. The configurations of the of the four foil trays are described below.³

Tray 1 (PNNL):

DU foil D-38-10-6, 0.5808 grams

HEU foil 8551-409, 0.0622 grams

Foil packet "22 Bare" (foils supplied by PNNL:

Cu(0.1551 g)+Fe(0.7922 g)+Co(0.01405 g)+Au(0.1244 g)+Ti(0.1577 g))

Foil packet "21 Cd" (supplied by PNNL: as above, but Cd cover:

Cu(0.1551 g)+Fe(0.7960 g)+Co(0.012386 g)+Au(0.1236 g)+Ti(0.1572 g))

Tray 2 (NCERC/LANL):

NCERC:

DU foil D-38-10-7, 0.5806 grams

HEU foil 8551-410, 0.0637 grams

LANL:

Au foil 11A, 0.1273 grams (sample ID 4116)

Pu foil JX-2229-D5, 0.3899 grams (Ni-clad) (sample ID 4113)

Tray 3 (LANL):

HEU foil 8551-408, 0.0638 grams (sample ID 4111)

DU foil D-38-10-5, 0.5803 grams	(sample ID 4112)
Ga sample 0.06087 grams of Ga_2O_3	(sample ID 4114)
Ir sample 0.10745 grams of K_2IrCl_6	(sample ID 4115)

Tray 4 (Empty)

The samples containing the Ir, Ga, both PNNL packs, and the Pu were wrapped in an additional aluminum foil to help ensure no compromise of the foil contents. The Comet assembly with the Zeus experimental configuration described above was run at an average power of about 2.3KW on September 8, 2011 for 3955 seconds as measured on the linear channel #2 (see Fig. 3). Note that linear channel #2 did not autorange to the next scale (blue dots), so that the current in linear channel #2 was adjusted based on the measured current in linear channels #1 and #3. The zero-time (ZT) corresponding to the end of bombardment (EOB) was 251.9576 GMT in Julian day decimal time. The foils were recovered late in the morning of September 12, 2011 (~3.75 days after EOB). The dose rate from the sides of Comet fuel was 110 mR/h at 1 foot on Monday morning at 9 AM when the radiological control technicians (RCTs) did the building reentry.³ The average power rate was inferred from post irradiation analysis of the HEU foils assuming a flat radial power distribution across the core. During recovery, the irradiation foils were placed on aluminum sample plates and covered with thin Mylar using double-sided sticky tape. These plates were then placed in plastic sample holders and double bagged.

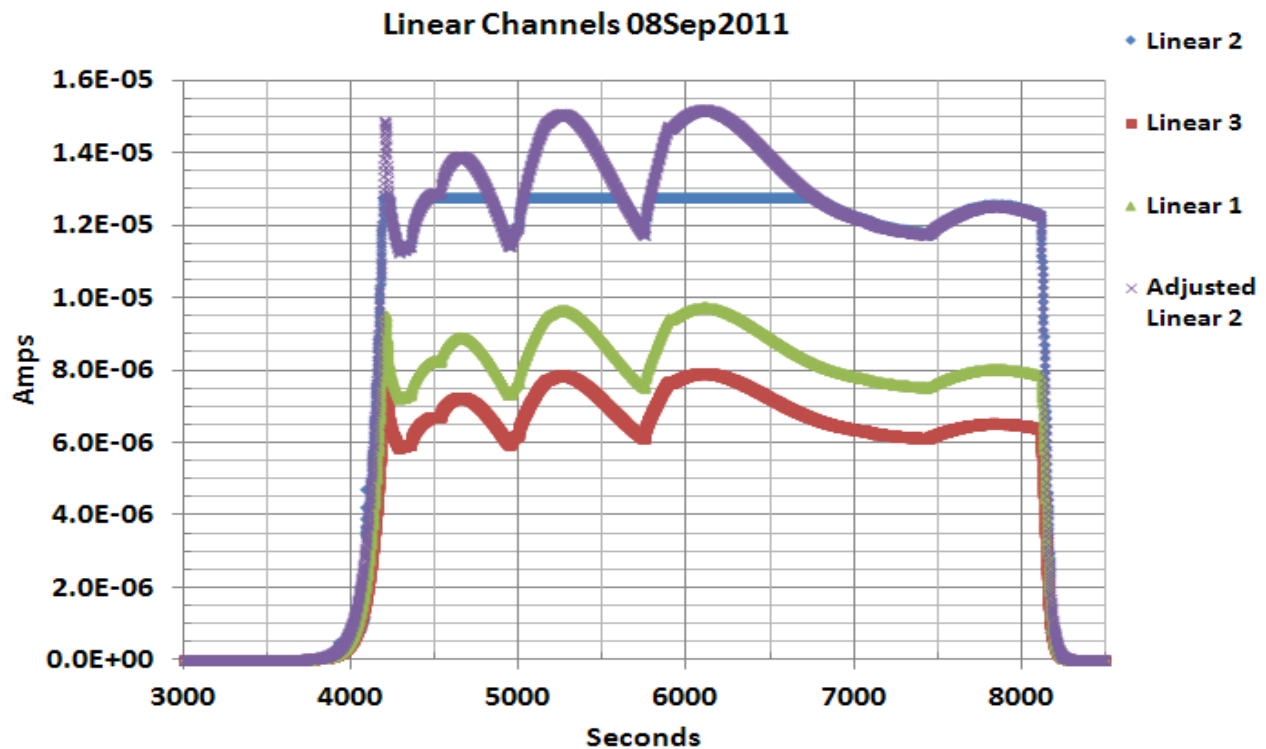


Figure 3. Measured current during the high-power Comet run in three Ion Chambers. Linear channel #2 is approximately 10-ft from the assembly.

Table I. Initial fission estimates based on gamma spec at DAF counting room.

Sample ID	Foil Mass (mg)	Fissions/g Foil	Total Fissions
4111	63.8	2.50E+12	1.60E+11
4112	580.3	2.20E+11	1.28E+11
4113	389.9	3.20E+12	1.25E+12

II.C. Radiochemistry

Most of the foils arrived at LANL on September 20, 2011 and were delivered to the Alpha Wing at TA-48 Building RC-1. The irradiated ^{239}Pu sample arrived on the afternoon of Wednesday, September 21, 2011. The dose reading on the first shipping container was 1.2 mRem/hr at contact prior to shipping on September 13, 2011. Dose rate readings were taken on individual samples and are shown in Table II. Also listed in the table are the LANL shot numbers assigned to the individual samples, and the mass of the materials. The samples were shipped in a slip-top can inside a Type A container with a Tamper Indicating Device (TID). After the TID was removed, the samples were unpackaged and sent to the count room for an overnight assay using gamma spectroscopy. Each sample had been sealed in a plastic container and placed inside a zip-lock bag for shipping. A photo of the samples after unpacking is shown in Fig. 4.

Table II. Sample target information.

Target	Sample ID	Target Mass (mg)	Dose Rate at Contact (mRem/hr)
U-235	4111	63.8	1.8
U-238	4112	580.3	1.4
Pu-239	4113	389.9	
Ga (Ga_2O_3)	4114	60.87	0
Ir (K_2IrCl_6)	4115	107.45	0.3
Au	4116	127.3	0.3



Figure 4. Photograph of samples 4111, 4112, 4114, 4115 and 4116.

The foils were given initial gamma-ray counts on HPGe detectors while still on the original sample plates. It was decided that the Pu, HEU, and DU samples would be dissolved, and then the standard suite of radiochemical analysis performed. The two uranium foils were returned to the Alpha Wing the morning of Wednesday, September 21 for dissolution. The foils were removed from their mounts by cutting away the mylar and dropping the foils into 600 mL Teflon beakers for dissolution. The foils were dissolved using concentrated HNO₃ and HCL. A small amount of fuming HNO₃ was needed to complete the dissolution due to small amount of oxide that had formed on the foils. The resulting solutions were diluted to ca. 100 mL in 4 M HNO₃ in 125 mL Teflon bottles. 5 mL aliquots of the "A" solutions were prepared, weighed, and delivered to the count room in 20 mL plastic scintillation vials to be used for gamma spectroscopy. These 5 mL aliquots were then gamma counted on HPGe detectors for about a week. 80 mL aliquots were prepared for the sequential separation and moved to the Actinide Research Facility (ARF). Aliquots were prepared for uranium and neptunium assays and delivered to the separation chemists. The sequential separation procedure was completed on Thursday, September 22.

The plutonium foil was returned to the Alpha Wing the morning of Thursday September 22 for dissolution. The mylar was cut away from the sample and the sample moved to a large petri dish. The nickel-coated plutonium disk was wrapped in aluminum foil, which was removed from the sample using forceps. The disk was placed into a 600 mL Teflon beaker for dissolution. The nickel coating was dissolved using 6 M HCL at ca. 200 °C. The plutonium disk was then dissolved using concentrated HNO₃, fuming HNO₃ and HF at 280 °C. The resulting solution was concentrated to near dryness and brought up in 100 mL of 4M HNO₃ in a Teflon bottle. A 5 mL aliquot of the resulting "A" solution was prepared for the count room for gamma assay and an 80 mL aliquot was prepared for the sequential separation. An 80 mL reagent blank was also prepared in 4M HNO₃. The sequential separation procedure for the ²³⁹Pu foil experiment was carried out in the Alpha Wing. The samples coming off of the sequential separation were delivered to the separation chemists on Friday, September 23.

The whole "A" solution aliquots were analyzed for several fission products (⁹⁹Mo, ^{99m}Tc, ⁹⁵Zr, ¹⁰³Ru, ¹³²Te, ¹⁴⁰Ba, ¹⁴¹Ce, ¹⁴⁷Nd) using gamma spectroscopy. The 10-element plus lanthanides sequential separation provided fractions for purification including Ba/Sr, Zr, Mo, Cs, Ag, Cd, Sm, Eu, Tb, U, Np, and Pu. From these sequential fractions, separated samples of Mo, Ag, Sm, Eu, Tb, and Np were prepared and counted for the ²³⁵U foil experiment, 4111. A ²³⁷U sample was prepared from a 5 mL aliquot of the "A" solution. From the sequential fractions in the ²³⁸U experiment (4112), separated samples of Mo, Ag, Sm, Eu, and Tb were prepared and counted. From the sequential fractions in the ²³⁹Pu experiment (4113), separated samples of Mo, Ag, Sm, Eu, and Tb were prepared and counted. In all cases, the Ba/Sr, Zr, Cd, Cs, and Pu fractions were held for further analysis if requested. Molybdenum was separated, purified, and mounted as MoO₃. Silver was separated, purified, and electroplated as metal. The lanthanides were separated, purified, and mounted as Ln₂O₃.

A ²³⁷U sample and a ²³⁹Np sample were prepared from a 1 mL aliquots of the "A" solution for the 4111 and 4112. Separated samples of ²³⁷U were prepared from these aliquots as described above in the ²³⁵U and ²³⁸U foil experiments. Separated samples of ²³⁹Np were prepared from the Np cut off from the

sequential separation ^{235}U foil experiment, and from an aliquot of the “A” solution in the ^{238}U foil experiment.

The separated samples were beta and gamma counted for the fission products and actinides. The isotopes of the uranium foils (4111 and 4112) were analyzed using inductively-coupled mass spectrometry (ICP-MS). The iridium foil was also chemically dissolved, separated, and analyzed using a combination of gamma spectroscopy and X-ray counting. The gold and gallium foils were only measured by gamma spectroscopy of the whole foils. Most of the reported results are in terms of atoms per gram of “A” solution, so that they are in comparable basis. The results are corrected for decay during counting and irradiation. However, the values are not corrected for gamma-ray self-absorption or summing effects. The results for the PNNL and DAF foils are not presented in this report.

III. EXPERIMENTAL RESULTS

III.A. Gold (4116)

The gold foil, serial number 11A, had a mass of 0.1273 grams. Gold is often used as an activation foil, because of the large neutron capture cross section of ^{197}Au . Gold has a high absorption resonance at 5 eV, and can be used in conjunction with a Cd covered Au foil to estimate the thermal neutron flux. Unfortunately, there were only a limited number of irradiation positions, so the Cd covered Au foil was removed before irradiation. The gold foil was measured using gamma spectroscopy at LANL, and the only isotopes of gold observed were ^{196}Au and ^{198}Au . Table III shows the determined activities and atoms per gram of foil. The values reported are the average of four separate measurements made on different gamma-ray counting systems.

Table III. Measured activities and atoms per gram of foil for gold isotopes.

Isotope	DPM @ EOB	Atoms/g foil @ EOB
Au-196	$2.51\text{E}+04 \pm 7.8\%$	$2.53\text{E}+09 \pm 7.8\%$
Au-198	$1.08\text{E}+07 \pm 4.3\%$	$4.76\text{E}+11 \pm 4.3\%$

III.B. Iridium (4115)

The iridium foil consisted of 0.10745 grams of K_2IrCl_6 wrapped in aluminum foil. The K_2IrCl_6 was dissolved and the iridium was chemically separated using a procedure outlined in LA-1721.⁵ The isotopes ^{189}Ir , ^{190}Ir , and ^{192}Ir were determined by gamma spectroscopy, and $^{193\text{m}}\text{Ir}$ was determined by X-ray counting. The iridium results are shown in Table IV. It should be mentioned that based on the low neutron flux and long decay time, the maximum sample size available was used for this analysis. The activities of ^{189}Ir and ^{190}Ir were also approaching our detection limits by the time they reached the counters. The value for ^{189}Ir is reported as the estimate upper limit for what the measurement instrument could observe. The values reported are per gram of precipitated sample because there is no equivalent “A” solution for the iridium chemistry.

III.C. Gallium (4114)

The gallium foil consisted of 0.06087 grams of Ga_2O_3 wrapped in aluminum foil. ^{72}Ga was the only isotope measured because the other gallium isotopes had short half-lives relative to the recovery time. The recovery time typically needs to be on the order of the half-life in order to measure it.³ The only usable result for the gallium foil was a short spectrum obtained at NCERC counting room. By the

Table IV. Measured activities and atoms per gram of foil for iridium isotopes.

Isotope	Atoms / g sample @ EOB
Ir-189	7E+06 (limit)
Ir-190	$8.7\text{E}+08 \pm 50.3\%$
Ir-192	$1.215\text{E}+11 \pm 0.7\%$
Ir-193m	$6.07\text{E}+10 \pm 1.5\%$

time the foils reached LANL, ~10 days after EOB, no ^{72}Ga was observed. Table V shows the results from the gamma spectroscopy measurements at NCERC. It should be noted that the uncertainties on this measurement are high because the counting statistics were low and the lack of the appropriate calibration curve for the counting geometry. The efficiency curve for this counting geometry was estimated using the KMESS code.

Table V. Measured activity and atoms per gram of foil for gallium.

Isotope	DPM @ EOB	Atoms/g foil @ EOB
Ga-72	$2.4\text{E}+04 \pm 21\%$	$4.8\text{E}+08 \pm 21\%$

III.D. Plutonium (4113)

The Pu foil, serial number JX-2229-D5 (Ni-clad), had a mass of 0.3899 grams, and was dissolved into an "A" solution with a total mass of 119.074 grams. The 5 mL "A" solution aliquot had a mass of 5.548 grams, and was gamma counted for about a week. The results from these measurements are shown in Table VI.

Table VI. Measured atoms per gram of "A" solution and R-values for the Pu foil by gamma spec.

Isotope	Atoms/g "A" @ EOB	R
Mo-99	$6.7\text{E}+08 \pm 14\%$	1.002
Zr-95	$5.1\text{E}+08 \pm 11\%$	0.703
Ru-103	$7.16\text{E}+08 \pm 6.2\%$	2.132
Te-132	$6.3\text{E}+08 \pm 18\%$	1.310
Ba-140	$6.72\text{E}+08 \pm 9.4\%$	0.985
Ce-141	$1.02\text{E}+09 \pm 6.0\%$	1.548
Nd-147	$2.6\text{E}+08 \pm 23\%$	1.070

The large uncertainties in Table VI are primarily due to the samples arriving at LANL so late after EOB. This made using whole-solution gamma spectroscopy to measure several of the isotopes difficult, because of the low activities and poor counting statistics. The gamma spectroscopy estimated number of fissions per gram of "A" solution based on ^{99m}Tc is $1.1\text{E}+10 \pm 14\%$, and the total number of fissions based on ^{99m}Tc is $1.3\text{E}+12 \pm 14\%$. The cumulative fission chain yield used in this conversion was for thermal fissions in the in ^{235}U of ^{99}Mo , namely 6.11%.⁶ For comparison, the cumulative fission chain yield for fast fissions in ^{239}Pu of ^{99}Mo is 5.98%.⁶ The ^{99}Mo activity was low enough that the fission per gram by gamma spectroscopy had to be estimated assuming secular equilibrium with the ^{99m}Tc daughter. Another issue encountered in gamma counting was the large amount of ^{241}Am present in the sample. This set limitations on our count lengths in order to not overload the memory in our spectrometers.

The radiochemical separations yielded better results than the gamma spectroscopy for the Pu foil, as shown in Table VII. The separated fission products were measured by gas-flow proportional β -counters. The β -counting estimated number of fissions per gram of "A" solution based on the ^{99}Mo is $1.21\text{E}+10 \pm 0.3\%$, and the total number of fissions is $1.44\text{E}+12 \pm 0.3\%$. The fission estimate from β -counting should be taken as the "best" value, because of the higher precision of the measurements from separated samples. The actinide composition of the Pu foil was not analyzed.

Table VII. Measured atoms per gram of "A" solution and R-values for the Pu foil by β -counting.

Isotope	Atoms / g "A" @ EOB	R
Mo-99	$7.39\text{E}+8 \pm 1.4\%$	-
Ag-111	$3.93\text{E}+7 \pm 1.5\%$	18.68
Sm-153	$5.58\text{E}+7 \pm 2.2\%$	2.92
Eu-156	$2.03\text{E}+7 \pm 2.8\%$	11.24
Tb-161	$5.7\text{E}+5 \pm 13.7\%$	55.2

III.E. Depleted Uranium (4112)

The DU foil, serial number D-38-10-5, had a mass of 0.5803 grams, and was dissolved into an "A" solution with a total mass of 116.679 grams. The 5 mL "A" solution aliquot had a mass of 5.715 grams, and was counted for about a week. The results from those measurements are shown in Table VIII.

Table VIII. Measured atoms per gram of "A" solution and R-values for the DU foil by gamma spec.

Isotope	Atoms/g "A" @ EOB	R
Mo-99	$7.84\text{E}+07 \pm 5.7\%$	1.002
Zr-95	$6.03\text{E}+07 \pm 6.1\%$	0.720
Ru-103	$7.09\text{E}+07 \pm 5.2\%$	1.815
Te-132	$6.15\text{E}+07 \pm 7.9\%$	1.095
Ba-140	$6.69\text{E}+07 \pm 5.5\%$	0.843
Ce-141	$6.46\text{E}+07 \pm 5.1\%$	0.847
Nd-147	$3.01\text{E}+07 \pm 7.3\%$	1.068

The gamma spectroscopy estimated number of fissions per gram of "A" solution based on the ^{99}Mo is $1.28\text{E}+09 \pm 5.7\%$, and the total number of fissions based on the ^{99}Mo is $1.50\text{E}+11 \pm 5.7\%$. The cumulative fission chain yield used in this conversion was also for thermal fissions in ^{235}U of ^{99}Mo . For comparison, the cumulative fission chain yield for fast fissions in ^{238}U of ^{99}Mo is 6.17%.⁷ The uncertainties are also large for several isotopes, because of the long decay time between EOB and count time. Another difficulty encountered in analyzing the DU by gamma spectroscopy was the amount of ^{239}Np present in the sample. ^{239}Np has a large distribution of gamma-ray energies, and many interfere with the gamma-ray energies from other fission products.

The results from the radiochemical separation of the DU foil are presented in Table IX. The separated fission products were also measured by gas-flow proportional β -counters. The β -counting estimated number of fissions per gram of "A" solution based on the ^{99}Mo is $1.29\text{E}+09 \pm 0.3\%$, and the total number of fissions is $1.50\text{E}+11 \pm 0.3\%$. Notice the ^{99}Mo estimates agree well with the quoted uncertainties from gamma spectroscopy. The fission estimate from β -counting should be taken as the "best" value, because of the higher precision of measurements from separated samples.

Table IX. Measured atoms per gram of "A" solution and R-values for the DU foil by β -counting.

Isotope	Atoms / g "A" @ EOB	R
Mo-99	$7.85\text{E}+7 \pm 1.4\%$	-
Ag-111	$8.36\text{E}+5 \pm 1.5\%$	3.74
Sm-153	$5.64\text{E}+6 \pm 2.6\%$	2.78
Eu-156	$1.09\text{E}+6 \pm 2.8\%$	5.67
Tb-161	$3.3\text{E}+5 \pm 14.3\%$	304.61

The uranium composition was also analyzed using ICP-MS. The isotopic composition of the DU foil is shown in Table X. Notice the amount of ^{238}U is greater than in natural uranium (99.3%) as expected. The amount of ^{237}U and ^{239}Np were also determined using separated samples by gamma spectroscopy and are shown in Table XI.

Table X. Uranium composition of the DU foil.

Isotope	Composition [%]
U-234	$1.1\text{E}-04 \pm 17.8\%$
U-235	$2.63\text{E}-01 \pm 1.5\%$
U-236	$2.8\text{E}-03 \pm 10.7\%$
U-238	$9.9733\text{E}+01 \pm 0.004\%$

Table XI. ^{237}U and ^{239}Np atoms per gram of "A" after irradiation in the DU foil.

Isotope	Atoms / g "A" @ EOB
U-237	$4.68\text{E}+07 \pm 5.1\%$
Np-239	$1.42\text{E}+09 \pm 3.5\%$

III.F. Highly-Enriched Uranium (4111)

The HEU foil, serial number 8551-408, had a mass of 0.0638 grams, and was dissolved into an "A" solution with a total mass of 116.166 grams. The 5 mL "A" solution aliquot had a mass of 5.663 grams, and was gamma counted for a week. The results from these measurements are shown in Table XII.

Table XII. Measured atoms per gram of "A" solution and R-values for the HEU foil by gamma spec.

Isotope	Atoms/g "A" @ EOB	R
Mo-99	$7.94\text{E}+07 \pm 9.9\%$	1.002
Zr-95	$8.11\text{E}+07 \pm 5.8\%$	0.955
Ru-103	$4.26\text{E}+07 \pm 5.4\%$	1.075
Te-132	$6.28\text{E}+07 \pm 7.9\%$	1.104
Ba-140	$8.33\text{E}+07 \pm 9.3\%$	1.036
Ce-141	$1.09\text{E}+08 \pm 5.1\%$	1.406
Nd-147	$2.83\text{E}+07 \pm 7.6\%$	0.994

The estimated number of fissions per gram of "A" solution based on ^{99}Mo is $1.30\text{E}+09 \pm 9.9\%$, and the total number of fissions based on the ^{99}Mo is $1.51\text{E}+11 \pm 9.9\%$. The cumulative fission chain yield used in the conversion was also for thermal fissions in ^{235}U of ^{99}Mo . The uncertainties are also large for several isotopes, because of the long decay time between EOB and count time.

The results from the radiochemical separation of the HEU foil are presented in Table XIII. The separated fission products were also measured by gas-flow proportional β -counters. The β -counting estimated number of fissions per gram of "A" solution based on ^{99}Mo is $1.423\text{E}+09 \pm 0.2\%$, and the total number of fissions is $1.653\text{E}+11 \pm 0.2\%$. The fission estimate from β -counting should be taken as the "best" value, because the higher precision of measurements from separated samples.

Table XIII. Measured atoms per gram of "A" solution and R-values for the HEU foil by β -counting.

Isotope	Atoms / g "A" @ EOB	R
Mo-99	$8.69\text{E}+7 \pm 1.4\%$	-
Ag-111	$4.86\text{E}+5 \pm 1.5\%$	1.96
Sm-153	$2.77\text{E}+6 \pm 2.9\%$	1.23
Eu-156	$3.29\text{E}+5 \pm 2.3\%$	1.55
Tb-161	$1.5\text{E}+4 \pm 31\%$	12.23

The uranium composition was also analyzed using ICP-MS. The isotopic composition of the HEU foil is shown in Table XIV. Notice that the enrichment appears to be about 93.2% ^{235}U . The amount of ^{237}U and ^{239}Np were also determined using the separated samples by gamma spectroscopy and are shown in Table XV. The amount of ^{237}U is reported as below the detection limit (BDL).

Table XIV. Uranium composition of the HEU foil.

Isotope	Composition [%]
U-234	$8.92\text{E-}01 \pm 0.7\%$
U-235	$9.324\text{E+}01 \pm 0.03\%$
U-236	$5.57\text{E-}01 \pm 1.2\%$
U-238	$5.31\text{E+}00 \pm 0.5\%$

Table XV. ^{237}U and ^{239}Np atoms per gram of "A" after irradiation in the HEU foil.

Isotope	Atoms / g "A" @ EOB
U-237	BDL
Np-239	$8.00\text{E+}06 \pm 7.6\%$

III.G. Fission Ratios

For the LANL samples, there were two fissile foils (HEU and Pu) and one fissionable foil (DU) irradiated during this experiment. Fission ratios are important because they provide information regarding the neutron spectrum for a particular critical experiment. To determine these ratios, the information provided in the previous section is used.

For the DU foil, the fissions per gram of "A" solution is reported as $1.29\text{E+}09$ and the mass of solution "A" (that includes the entire DU foil) was 116.679 grams, so the total fissions for the entire DU foil dissolved in "A" solution were $1.505\text{E+}11$. The mass of the DU foil was reported as 0.5803 grams and using 99.733 % ^{238}U by weight, the fissions per gram of ^{238}U were $1.505\text{E+}11/(0.5803*0.99733)=2.60\text{E+}11$. There are $0.00252973\text{E+}24$ atoms $^{238}\text{U}/(\text{g } ^{238}\text{U})$ so the fissions/(atom ^{238}U) is $2.60\text{E+}11$ fissions/(atom ^{238}U) = $1.027\text{E+}14$ fissions/($10\text{E+}24$ atoms ^{238}U).

For the HEU foil, the fissions per gram of "A" solution is reported as $1.423\text{E+}09$ and the mass of solution "A" (that includes the entire HEU foil) was 116.166 grams, so the total fissions for the entire HEU foil dissolved in "A" solution were $1.653\text{E+}11$. The mass of the HEU foil was reported as 0.0638 grams and using an enrichment of 93.24% ^{235}U by weight, the fissions per gram of ^{235}U were $1.653\text{E+}11/(0.0638*0.9324) = 2.779\text{E+}12$. There are $0.00256209\text{E+}24$ atoms $^{235}\text{U}/(\text{g } ^{235}\text{U})$ so the fissions/(atom ^{235}U) is $2.779\text{E+}12$ fissions/(atom ^{235}U) = $1.085\text{E+}15$ fissions/($10\text{E+}24$ atoms ^{235}U).

Finally, for the Pu foil, the fissions per gram of "A" solution is reported as $1.21\text{E+}10$ and the mass of solution "A" (that includes the entire Pu foil) was 119.074 grams, so the total fissions for the entire Pu foil dissolved in "A" solution were $1.44\text{E+}12$. The mass of the Pu foil was reported as 0.3899 grams and

using an enrichment of 95.82% ^{239}Pu by weight, the fissions per gram of ^{239}Pu were $1.44\text{E}+12/(0.3899*0.9582) = 3.854\text{E}+12$. There are $0.0025192\text{E}+24$ atoms $^{239}\text{Pu}/(\text{g } ^{239}\text{Pu})$ so the fissions/(atom ^{239}Pu) is $3.854\text{E}+12 \text{ fissions}/(\text{g } ^{239}\text{Pu})/(0.0025192\text{E}+24 \text{ atoms } ^{239}\text{Pu}/(\text{g } ^{239}\text{Pu})) = 1.530\text{E}+15 \text{ fissions}/(10\text{E}+24 \text{ atoms } ^{239}\text{Pu})$.

As stated in the previous section, the thermal fission yield of ^{235}U was used to convert the count rates from molybdenum to fission rates. Because this critical experiment is a fast system, fast fission yields must be used with the appropriate fission foil. Thus, the total fissions per gram were estimated based on the ^{99}Mo activity and the fast fission yields of 6.17% for ^{238}U , 5.94% for ^{235}U , 5.98% for ^{239}Pu .⁶

For the DU foil, the fissions per gram of ^{238}U given the new conversion factor is $2.60\text{E}+11*0.0611/0.0617 = 2.575\text{E}+11$. The fissions per atom of ^{238}U is $1.027\text{E}+14 \text{ fissions}/(10\text{E}+24 \text{ atoms } ^{238}\text{U})*0.0611/0.0617 = 1.017\text{E}+14/(10\text{E}+24 \text{ atoms } ^{238}\text{U})$.

For the HEU foil, the fissions per gram of ^{235}U given the new conversion factor is $2.779\text{E}+12*0.0611/0.0594 = 2.859\text{E}+12$. The fissions per atom of ^{235}U is $1.085\text{E}+15 \text{ fissions}/(10\text{E}+24 \text{ atoms } ^{235}\text{U})*0.0611/0.0594 = 1.116\text{E}+15/(10\text{E}+24 \text{ atoms } ^{235}\text{U})$.

Finally, for the Pu foil, the fissions per gram of ^{239}Pu given the new conversion factor is $3.854\text{E}+12*0.0611/0.0598 = 3.937\text{E}+12$. The fissions per atom of ^{239}Pu is $1.530\text{E}+15 \text{ fissions}/(10\text{E}+24 \text{ atoms } ^{239}\text{Pu})*0.0611/0.0598 = 1.563\text{E}+15/(10\text{E}+24 \text{ atoms } ^{239}\text{Pu})$.

The total fissions per gram and fissions per atom for each of the fission foils are presented in Table XVI. Additionally, the observed fission ratios (spectral indices) for this experiment and other critical assemblies are shown in the same table.

Table XVI. Total fissions/gram, fissions /atom, and fission ratios.

Zeus all oralloy experiment						
Total number of fissions/gram						
²³⁸ U	²³⁵ U		²³⁹ Pu			
2.575E+11	2.859E+12		3.937E+12			
Total number of fissions/(10E+24 atoms)						
²³⁸ U	²³⁵ U		²³⁹ Pu			
1.017E+14	1.116E+15		1.563E+15			
Critical assembly	_____		_____		_____	
Zeus all oralloy	11.10 mass basis	10.97 atom basis	1.38 mass basis	1.40 atom basis	15.29 mass basis	15.37 atom basis
Godiva Bare Oy-94 ⁷	6.5 mass basis	-	1.42 mass basis	-	9.23 mass basis	-
Topsy (Oy-94 in thick U) ⁷	7.3 mass basis	-	1.40 mass basis	-	10.22 mass basis	-

The Godiva assembly, also known as Lady Godiva, was a bare 94% enriched ^{235}U metal spherical critical assembly. It is expected that the neutron spectrum in this assembly approached that of a pure ^{235}U fission spectrum. On the other hand, Topsy was an assembly with a pseudospherical 94% ^{235}U metal core surrounded by a thick natural uranium reflector. For the Topsy assembly, the neutron spectrum should be softer when compared to Godiva because the reflected neutrons would have slightly less energy than those neutrons produced during the fission process. For the Zeus all alloy experiment, the neutron spectrum should be the softest of the three because the neutrons reflected back from the copper reflector would have less energy than those reflected back from natural uranium. As seen in Table XVI, the $\sigma_f(^{235}\text{U})/\sigma_f(^{238}\text{U})$ and $\sigma_f(^{239}\text{Pu})/\sigma_f(^{238}\text{U})$ ratios are the lowest for the Godiva assembly followed by Topsy and the Zeus all alloy experiment, which confirm our assumptions stated above.

From Table XVI, the fission ratio, $\sigma_f(^{238}\text{U})/\sigma_f(^{235}\text{U})$, is 0.0900 on mass basis and 0.0912 on an atom basis. The reported measured values do not attempt to correct for the ^{235}U fission in the DU foil or the ^{238}U fission in the HEU foil. These measured values also do not attempt to correct for self-shielding in the foils.

IV. Computational Model

IV.A. Assembly and HEU Plates

The starting point for the computational model was the fifth Zeus experiment, HEU-MET-FAST-073 in the International Handbook of Evaluated Criticality Safety Benchmark Experiments.¹ The main differences between IER-163 and HEU-MET-FAST-073 were: 1) IER-163 had two HEU plates below the diaphragm and six above; 2) the arrangement of plates (i.e., which plates were where) was of course different; 3) the arrangement of copper reflector blocks was different; 4) in IER-163 the room walls were closer; and 5) IER-163 had an aluminum sample holder⁸ and 12 irradiation foils between the bottom reflector and the bottom HEU plate. The detailed MCNP input deck listed in Appendix B of Ref. 1 was used and modified to account for these differences. Thick concrete room walls were added for IER-163.

Figure 5 (on the next page) shows a side view of IER-163 as installed on Comet. The support plate (the blue part at the bottom of Fig. 5 is 6 ft. above the concrete floor. Figure 6 (also on the next page) shows the sample holder, which was modeled in accordance with Ref. 8, and some of the copper parts.

The arrangement of HEU plates in IER-163 was provided by Bill Myers.⁹ Actual part dimensions and masses were obtained from an Excel spreadsheet of Jemima plate data also provided by Bill.¹⁰ Individual Jemima plate dimensions and masses (and therefore mass densities) are correct in the IER-163 MCNP model. However, HEU material definitions are not; the plate-specific HEU-MET-FAST-073 material assignments were not updated to the IER-163 model.

IV.B. Irradiation Foils

Five irradiation foils were modeled: HEU, depleted uranium (DU), plutonium, iridium, and gold. The composition of each foil is given in Table XVI. The HEU and DU compositions were obtained from Ref. 11 (Tables 14 and 10, respectively) and input as the weight percents appearing there; the numbers

03/06/12 11:59:00
zeus ier 163, with walls

```
probid = 03/06/12 11:58:46
basis: YZ
( 0.000000, 1.000000, 0.000000)
( 0.000000, 0.000000, 1.000000)
origin:
( 0.00, 0.00, 58.00)
extent = ( 65.00, 65.00)
```

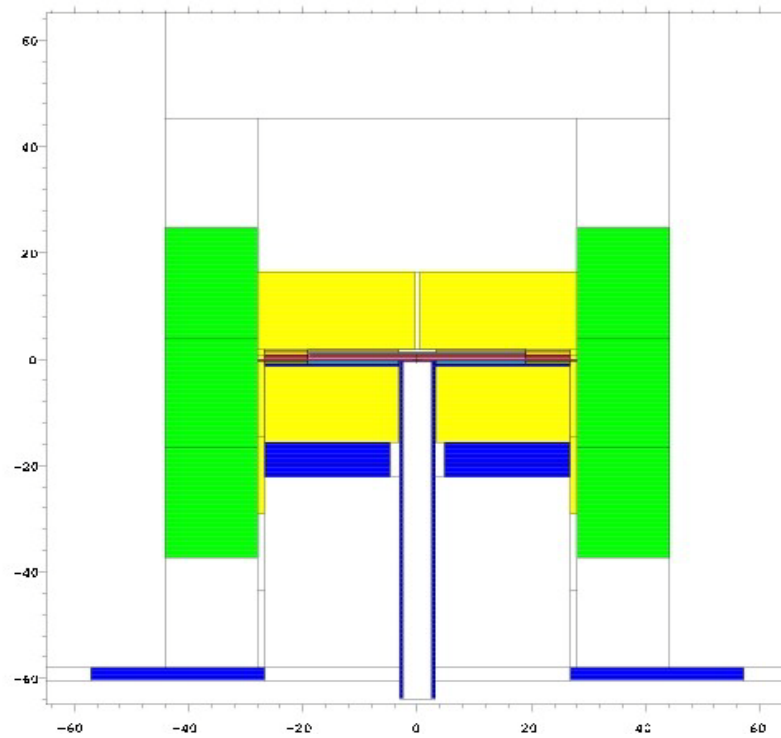


Figure 5. MCNP rendering of Comet containing IER-163.

03/09/12 08:29:34
zeus ier 163, with walls

```
probid = 03/09/12 08:12:53
basis: XY
( 1.000000, 0.000000, 0.000000)
( 0.000000, 1.000000, 0.000000)
origin:
( 0.00, 0.00, 56.76)
extent = ( 50.00, 50.00)
```

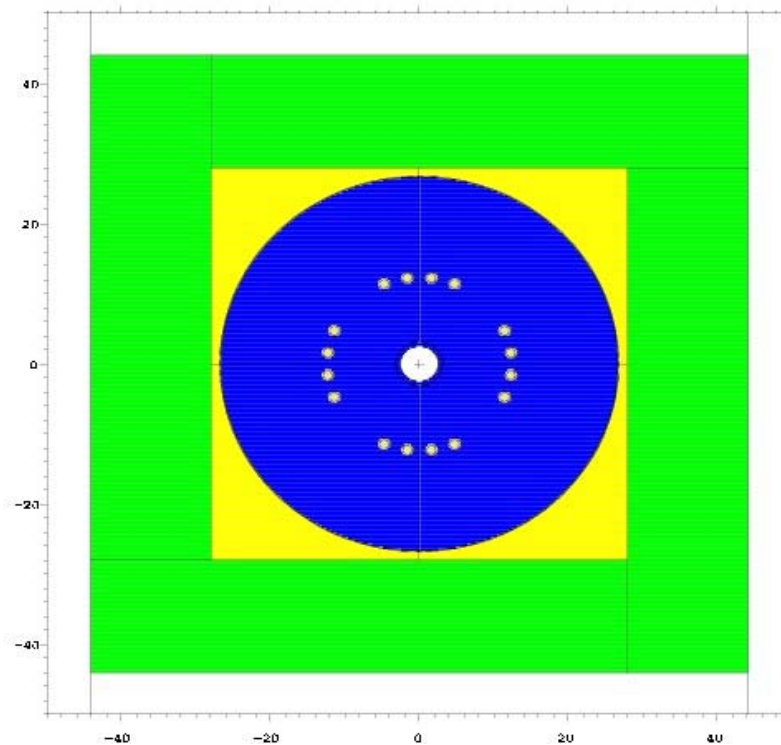


Figure 6. MCNP rendering of the aluminum sample holder on Comet

reported here are normalized and converted to atom fractions by MCNP. The enrichment of the HEU foil was¹¹ 93.24 %.

Table XVII. Foil Material Specifications.

Material	Isotope	Atom Fraction
HEU	²³⁴ U	8.96420E-03
	²³⁵ U	9.33022E-01
	²³⁶ U	5.55006E-03
	²³⁸ U	5.24642E-02
DU	²³⁴ U	1.11882E-06
	²³⁵ U	2.66358E-03
	²³⁶ U	2.82372E-05
	²³⁸ U	9.97307E-01
Plutonium	²³⁸ Pu	2.30858E-05
	²³⁹ Pu	9.35617E-01
	²⁴⁰ Pu	3.00703E-02
	²⁴¹ Pu	3.62083E-05
	²⁴² Pu	5.05581E-05
	²⁴¹ Am	7.25315E-04
	⁶⁹ Ga	2.01269E-02
	⁷¹ Ga	1.33507E-02
Iridium	³⁹ K	2.07923E-01
	⁴⁰ K	2.54328E-05
	⁴¹ K	1.42733E-02
	¹⁹¹ Ir	4.17159E-02
	¹⁹³ Ir	6.93952E-02
	³⁵ Cl	5.11833E-01
	³⁷ Cl	1.54833E-01
Gold	¹⁹⁷ Au	1.0

Contaminants were not included in Ref. 11. The plutonium composition was from gamma-ray spectrum analysis of a different foil¹² with 1% gallium (by weight) assumed; the numbers reported here are converted to atom fractions by MCNP. The plutonium in the foil was 96.86% ²³⁹Pu by weight¹²; the foil material including gallium was 95.82% ²³⁹Pu by weight. Contaminants were not included.

The foil masses, dimensions, and mass densities are listed in Table XVIII. The masses but not the dimensions of the foils are given in Ref. 11. The foil radii were obtained from Bob Rundberg.¹³ Thicknesses were calculated using the known masses and radii and the assumed densities.

Table XVIII. Foil Masses, Dimensions, and Densities.

Foil	Mass (g)	Radius (cm)	Thickness (cm)	Density (g/cm³)
HEU	0.0638	0.635	0.0026899	18.7236
DU	0.5803	0.635	0.0241739	18.95
Plutonium^a	0.3899	0.6223	0.0205306	15.61
Iridium (K₂IrCl₆)	0.10745	0.7	0.0218715	3.1914
Gold	0.1273	0.635	0.0052068	19.3

^a Parameters given are for plutonium only, not including the nickel cladding.

The density of the HEU and DU foils were “U.S. Average” HEU and “typical” DU from Ref. 14. The density of the plutonium foil was for typical delta-phase plutonium. The density of the iridium foil was arbitrarily taken to be 90% of the theoretical density¹⁵ of K₂IrCl₆, 3.546 g/cm³. Results for iridium were not sensitive to this choice; see Sec. IV.F.

A 0.005-in. cladding of nickel was modeled on the plutonium foil. Also, in the experiment, the iridium and Ni-clad plutonium foils were “wrapped in aluminum foil.”¹¹ To simulate this in the calculations, the iridium and Ni-clad plutonium foils were clad in 0.001-in. thick aluminum.

In the measurement, each of 12 sample locations held a different sample and four locations were empty. The calculations were done differently. In the calculations, each of the 16 sample locations held the *same* sample. This was done for variance reduction. The five calculations (one for each sample) each took about four hours (not counting extra studies); one calculation would have had to be run 16 times longer, or 64 hours total vs. 20 hours (and the extra studies, such as the iridium foil density study of Sec. IV.F, would not have been possible).

All calculations used 50 inactive cycles, 1200 active cycles, and 100,000 neutrons/cycle.

IV.C Criticality

Results obtained for k_{eff} using three cross-section sets are listed in Table XIX. The ENDF6 and ENDF7 values would be prompt critical. What is the cause of the mismatch between these computed values and the experimentally observed value of [$k_{eff} \approx 1.00085?$] The IER-163 computational model is extremely similar to the as-built configuration, but it is not perfect. (The calculations of Table XIX used the gold irradiation foils.)

Table XIX. k_{eff} for IER-163.	
Cross Sections	k_{eff}
ENDF5 (mostly .50c)	0.99781 ± 0.00006
ENDF6 (mostly .66c)	1.00840 ± 0.00006
ENDF7 (mostly .70c)	1.01195 ± 0.00006

As stated above, IER-163 is very similar to the “fifth Zeus configuration,” HEU-MET-FAST-073 (Ref. 1). The detailed model in Appendix B of Ref. 1 was rerun with ENDF5, ENDF6, and ENDF7 cross sections (using 1200 active cycles and 100,000 neutrons/cycle rather than 600 and 10,000 as in Ref. 1). Results, shown in Table XX, are similar to the results of Table XIX. Also, the first two entries are very similar to results for the simpler model (of Appendix A) in Table 37 of HEU-MET-FAST-073 (Ref. 1).

Table XX. k_{eff} for HEU-MET-FAST-073.	
Cross Sections	k_{eff}
ENDF5 (mostly .50c)	0.99680 ± 0.00006
ENDF6 (mostly .60c)	1.00851 ± 0.00006
ENDF7 (mostly .70c)	1.01199 ± 0.00006

Thus, the results of Table XIX for k_{eff} for IER-163 are consistent with what has been seen before, and the large k_{eff} seems to be due to the cross sections. Copper cross sections have been blamed for the discrepancy.¹ Using ENDF6 cross sections for copper in IER-163 gave $k_{eff} = 1.012$; using ENDF5 cross sections for copper in IER-163 gave $k_{eff} = 1.002$. Numerical tests have determined that though the effect on k_{eff} is large, the effect on the reaction-rate ratios discussed in this paper is negligible; these results are discussed in the sections that follow.

IV.D Computational Fission Ratio

MCNP was used to compute the volume average fission rate in the samples, including ^{235}U fission in the DU foil and ^{238}U fission in the HEU foil. Track-length tallies in the foil convolved with the fission cross section in the foil (F4/FM4 with reaction -6) were used. These results were converted to fission rates per gram of ^{235}U and $10\text{E}+24$ atom ^{235}U for the HEU foil and fission rates per gram of ^{238}U and $10\text{E}+24$ atom ^{238}U for the DU foil. Results are shown in Table XXI.

In summary, the measured fission ratio in IER-163 was $0.091 \pm 0.36\%$ (atom basis) but the computed fission ratio was $0.0795 \pm 0.252\%$. The error in the calculation is 12.6% or 22 standard deviations, and the calculation is too low compared to measurements. This result is consistent with a pattern that has been seen before. Skip Kahler¹⁶ has plotted the error in the calculated fission ratio as a function of the

measured value for several configurations of Topsy and Flattop-25. In the range of 0.07 to 0.10, errors of 16% to 9% have been observed, and the calculations are always too low.

Table XXI. Fission Rates for Uranium Foils.

Foil	Fissions/cm ³	Fissions/(g ²³⁵ U or ²³⁸ U) ^a	Fissions/(10E+24 atom ²³⁵ U or ²³⁸ U) ^a
HEU	8.88753E-05 ± 0.115%	5.09084E-06 ± 0.115%	1.98697E-03 ± 0.115%
DU	7.55240E-06 ± 0.225%	3.98544E-07 ± 0.225%	1.57964E-04 ± 0.225%
Ratio	Not Applicable	0.0783 ± 0.252%	0.0795 ± 0.252%

^a Uranium basis is ²³⁵U for the HEU foil and ²³⁸U for DU foil.

Before the experiment, the fission ratio was predicted¹⁷ to be 0.100. This prediction was based on a calculation of the fifth Zeus configuration (HEU-MET-FAST-073) that had fission-rate tallies in a fuel plate in the middle of the assembly (plate 5 inner). When it became clear that the samples would be placed at the bottom of the assembly rather than the middle, fission ratios of 0.090 (plate 1 inner) and 0.084 (plate 1 outer) were predicted.^{18, 19} These tallies convolved the neutron flux in the fuel plates with fission cross sections for pure ²³⁸U and ²³⁵U at the same atomic density (that of the fuel plate).¹⁸ This appears to be a classic case of getting the right answer for the wrong reason. When the same tallies are used in the actual samples (either HEU or DU) in the IER-163 model, the result is 0.0776.

To determine whether there is a spectral effect associated with changing the copper cross section (as there is an effect on k_{eff} ; see Sec. IV.C), the fission ratio was calculated when ENDF6 and ENDF5 cross sections were used for copper. Results are compared with using ENDF7 for copper in Table XXII. The difference between the use of ENDF7 and ENDF6 is 1.25 standard deviations; the difference between the use of ENDF7 and ENDF5 is 0.5 standard deviations. If there is a spectral effect, the precision of these calculations is not tight enough to show it.

Table XXII. Fission Ratio for Different Copper Cross Sections.

Cu Cross Sections	Fission Ratio ^a
ENDF7	0.0795 ± 0.252%
ENDF6	0.0790 ± 0.252%
ENDF5	0.0793 ± 0.252%

^a Atom basis.

An attempt was made to estimate the effect of self-shielding in the HEU and DU foils. There are two competing effects. Neutron capture in the foils attenuates the flux, but of course fission in the foils increases the flux. Simulations were run with voids in place of the samples but using the right material definitions to compute fission-rate tallies in the voids. (MCNP will apply reaction-rate cross sections for tallying wherever the user desires.) The idea is that the middle of the void cell will see the same flux that the surfaces do, unlike in the real foil. The resulting fission ratio was $0.0797 \pm 0.257\%$ (atom basis), statistically indistinguishable from the value of $0.0795 \pm 0.252\%$ obtained with the samples in place. If there is a self-shielding effect, the precision of these calculations is not tight enough to show it. It may be argued that the reported measured value of the fission rate should be adjusted upward by $0.0797/0.0795 - 1 = 0.25\%$. However, it is not clear that voiding the sample regions captures both effects of self-shielding. Adjusting the measured value based on these calculations is not recommended; these results are reported merely to demonstrate that the effect is very small.

IV.E Calculated Plutonium Ratios

The calculated fission rate in the plutonium foil was $9.44429\text{E-}05 \pm 0.101\%$ fissions/cm³. This equates to $6.314\text{E-}06 \pm 0.101\%$ fissions/(g ²³⁹Pu) or $2.50642\text{E-}03 \pm 0.101\%$ fissions/(10E+24 atoms ²³⁹Pu).

The measured and calculated ratios of the ²³⁹Pu fission rate to the ²³⁵U and ²³⁸U fission rates (on a mass basis) are compared in Table XXIII. The calculated ratio with respect to ²³⁵U fission is too small by 10.1%; the calculated ratio with respect to ²³⁸U fission is too large by 3.6%. As measured in standard deviations (Nσ), these differences are quite large.

Table XXIII. Plutonium Fission Ratios.^a

Ratio	Measured	Calculated	C/M	Nσ
²³⁹ Pu(n,f)/ ²³⁵ U(n,f)	$1.38 \pm 0.36\%$	$1.240 \pm 0.15\%$	0.899	20.5
²³⁹ Pu(n,f)/ ²³⁸ U(n,f)	$15.29 \pm 0.42\%$	$15.843 \pm 0.25\%$	1.036	5.3

^a Mass basis.

These results, combined with those of Sec. IV.D, suggest that the calculated ²³⁵U fission rate is too large and the calculated ²³⁸U fission rate is too small. In fact there is an interesting convergence. From Table XXIII, decreasing the ²³⁵U fission rate by 10.1% and increasing the ²³⁸U fission rate by 3.6% would cause the calculated plutonium ratios to match the measured values. Doing this would also cause the uranium fission ratio to change by a factor of $1.036/0.899 = 1.152$. Applying this factor to the calculated uranium fission ratio of 0.0795 (atom basis; Sec. IV.D) yields 0.0916, much closer to the measured value of 0.091.

IV.F Iridium Ratio

The measured iridium ratio $^{193}\text{Ir}(n,n')/^{191}\text{Ir}(n,\gamma)$ can be obtained from Ref. 11 as the ratio of the measured values of ^{193m}Ir and ¹⁹²Ir. The numbers appearing in Table 4 of Ref. 11 were corrected in a subsequent email.²⁰ The measured iridium ratio is $(6.04\text{E+}10 \pm 2.7\% \text{ atoms/[g precipitate]})/(1.23\text{E+}11 \pm 0.2\% \text{ atoms/[g precipitate]}) = 0.491 \pm 2.71\%$.

Calculated results are shown in Table XXIV. Reaction rates were computed using the foil's atom density as a multiplier. The ratio is thus multiplied by the ratio of the atom fractions of ^{193}Ir and ^{191}Ir in the foil from Table XVII, $6.93952\text{E-}02/4.17159\text{E-}02$. In addition, for historic reasons, "measured ^{193m}Ir values need to be multiplied by a factor of 2.0 before comparing with the simulations."²¹ Here, instead, the calculated ratio is divided by 2.0.

Reaction rates were computed using two sets of cross sections. The first was the "T16_RC_2004" dosimetry library (extension 04y). In this library, reactions 51 and 4 for ^{193}Ir both give the inelastic scattering to ^{193m}Ir , and reaction 102 for ^{191}Ir gives the neutron capture to ^{192}Ir .

The second set of cross sections used for iridium reaction rates was the ENDF7 transport library (extension 70c). In this set, reaction 102 for ^{191}Ir gives the neutron capture to ^{192}Ir . However, without other data, there is no means of computing the $^{193}\text{Ir}(n,n')^{193m}\text{Ir}$ reaction rate. Skip Kahler provided the other data necessary for this calculation.²² Skip computed a set of dose-response function cards (DE/DF in MCNP parlance) that give the fraction of all the inelastic reactions that lead to ^{193m}Ir ; in the simulation, this dose function is convolved with a reaction-rate tally that adds all of the inelastic reactions (51 through 89 plus 91).

Table XXIV. Iridium Results.

Cross Sections	$^{193}\text{Ir}(n,n')^{193m}\text{Ir}$	$^{191}\text{Ir}(n,\gamma)^{192}\text{Ir}$	Ir Ratio	C/M	N σ
Dosimetry (.04y)	$1.32937\text{E-}05 \pm 0.167\%$	$2.10171\text{E-}05 \pm 0.152\%$	$0.526 \pm 0.226\%$	1.072	2.4
ENDF7 (.70c)	$1.40621\text{E-}05 \pm 0.164\%$	$2.00798\text{E-}05 \pm 0.134\%$	$0.582 \pm 0.211\%$	1.186	6.3

^a Reaction rates are volume averages.

Table XXIV shows that the dosimetry set gives an iridium ratio that is too large by 7.2% or 2.4 standard deviations, while ENDF7 gives an iridium ratio that is too large by 18.6% or 6.3 standard deviations.

The iridium ratio was predicted¹⁷ to be 0.76 based on laying the fission ratio prediction of 0.10 (Sec. IV.D) on the semi-empirical fit to the historical LANL data,¹⁸ not on an MCNP calculation.

The $^{191}\text{Ir}(n,\gamma)$ reaction rate was surprisingly difficult to calculate because of enormous resonances between 0.3 and 200 eV. The cross section (from the dosimetry set and ENDF7) is plotted in Figure 7. For example, in this calculation, the variance of the variance (VOV) shot from 0.0038 to 0.0251 (in the tally fluctuation chart) because of a single 78.73-eV neutron scoring by tracking through the iridium sample. (The VOV recovered, but the slope of the probability density function did not.) Interestingly, the neutron was born at 2.726 MeV, was thermalized in the concrete wall, and survived multiple collisions in passing through the bottom (copper) reflector to reach the samples.

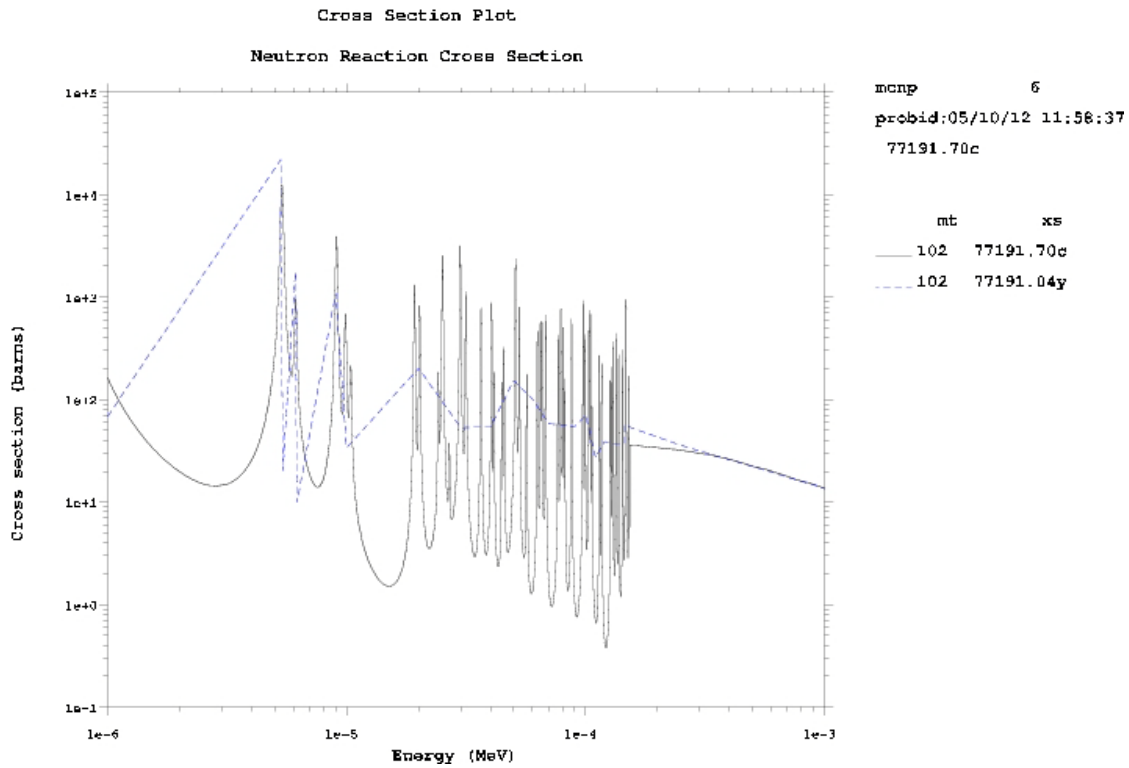


Figure 7. $^{191}\text{Ir}(n, \gamma)$ cross section.

To determine whether there is a spectral effect associated with changing the copper cross section (as there is an effect on k_{eff} ; see Sec. IV.C), the iridium ratio was calculated when ENDF6 and ENDF5 cross sections were used for copper. Results are compared with using ENDF7 for copper in Table XXV. The difference between the use of ENDF7 and ENDF6 is 1.4 standard deviations; the difference between the use of ENDF7 and ENDF5 is 1.6 standard deviations. There might be a small spectral effect on the iridium ratio, but these results are not conclusive. [The relatively large uncertainty in the ENDF6 result is due to the $^{191}\text{Ir}(n, \gamma)$ resonances as discussed above.]

Table XXV. Iridium Ratio for Different Copper Cross Sections.

Cu Cross Sections	Iridium Ratio ^a
ENDF7	$0.582 \pm 0.211\%$
ENDF6	$0.570 \pm 1.36\%$
ENDF5	$0.578 \pm 0.281\%$

^a Using ENDF7 reaction cross sections.

The actual mass density of the iridium sample was not measured. As stated in Sec. IV.B, the density was assumed to be 90% of the theoretical density. The effect of density was examined by examining the reaction rates and the ratio for sample densities of 85% and 95% of theoretical. Results are shown in Fig. 8. In this range of densities, the reaction rates are very linear, and the change in the ratio is statistically insignificant.

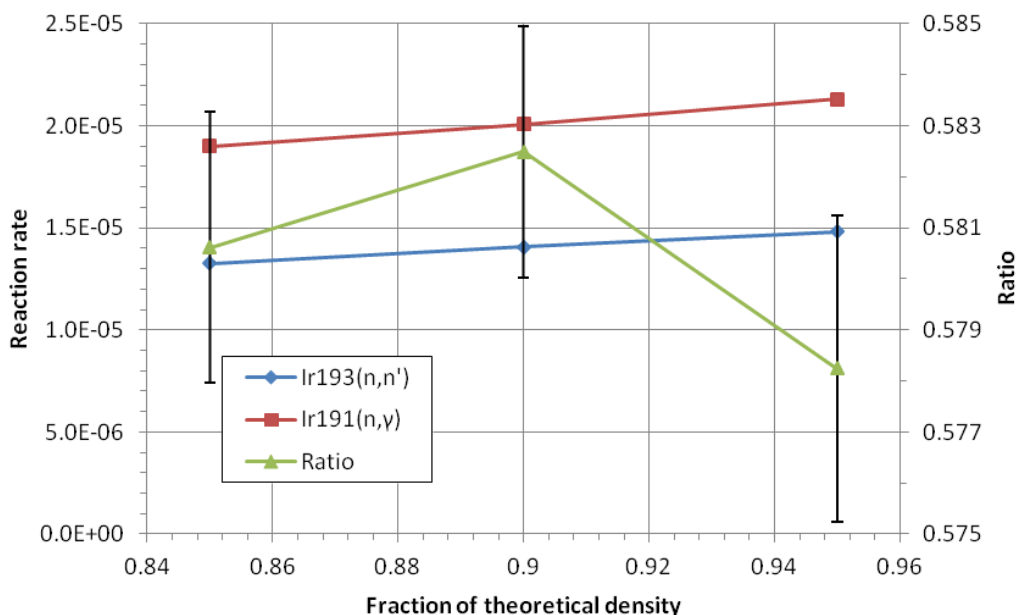


Figure 8. Iridium reaction rates and ratio as a function of foil density. 2σ uncertainties are shown.

IV.G Gold Ratios

The measured gold ratio $^{197}\text{Au}(n,2n)/^{197}\text{Au}(n,\gamma)$ can be obtained directly from Table 3 of Ref. 11 as the ratio of the measured values (atoms/g foil) of ^{196}Au and ^{198}Au , or $(2.53\text{E}+9 \pm 7.8\%)/(4.76\text{E}+11 \pm 4.3\%) = 5.32\text{E}-03 \pm 8.9\%$.

Calculated results are shown in Table XXVI. Reaction rates were computed using the ENDF7 transport library (extension 70c); reaction 16 gives (n, 2n) and reaction 102 gives (n, γ).

Table XXVI. Gold Results.	
Reaction or Ratio	Result ^a
$^{197}\text{Au}(n,2n)^{196}\text{Au}$	$8.23268\text{E}-08 \pm 3.39\%$
$^{197}\text{Au}(n,\gamma)^{198}\text{Au}$	$1.65487\text{E}-05 \pm 0.185\%$
Ratio	$4.97\text{E}-03 \pm 3.40\%$

^a Reaction rates are volume averages.

Table XXVI shows that the gold ratio is computed very accurately, within one standard deviation of the measured value, although the uncertainty of the measured value is relatively large.

It is also useful to look at the gold results as normalized by the ^{235}U fission rate. This was done on a mass basis. For the measured values, the atoms/(g foil) from Table 3 of Ref. 11 were divided by $2.779\text{E}+12$ fissions/(g ^{235}U) from Sec. IV.D. For the calculated values, the volumetric reaction rates of Table XXVI were divided by the gold density (19.3 g/cm^3 from Table XVIII) and divided by the calculated fission rate from Table XXI, $5.09084\text{E}-06$ fissions/(g ^{235}U). Results are shown in Table XXVII, where it is clear that the gold results are quite accurate, well within one standard deviation, although the uncertainty in the measured values is large.

Table XXVII. Gold Results Normalized by Fission.

Ratio	Measured	Calculated	C/M	N σ
$^{197}\text{Au}(n,2n)/^{235}\text{U}(n,f)$	$9.10\text{E}-04 \pm 7.80\%$	$8.38\text{E}-04 \pm 3.40\%$	0.920	0.73
$^{197}\text{Au}(n,\gamma)/^{235}\text{U}(n,f)$	$1.71\text{E}-01 \pm 4.30\%$	$1.68\text{E}-01 \pm 0.22\%$	0.983	0.37

It should be noted that decreasing the ^{235}U fission rate by 10.1%, as suggested in Sec. IV.E, improves the $^{197}\text{Au}(n,2n)/^{235}\text{U}(n,f)$ agreement, changing C/M to 1.02 and N σ to 0.21. However, it makes the $^{197}\text{Au}(n,\gamma)/^{235}\text{U}(n,f)$ agreement worse, changing C/M to 1.09 and N σ to 2.04.

An attempt was made to estimate the effect of self-shielding in the gold foil. As in Sec. IV.D, the problem was run with void where the foil should have been, but with reaction-rate tallies in the void. Results are shown in Table XXVIII. Replacing the gold with void removes the physical production of (n,2n) neutrons, but in the problem that included the gold, out of a total weight of 1.47×10^{-2} neutrons entering the gold foils, a total weight of 1.67×10^{-8} neutrons were produced from (n,2n) reactions (from the neutron weight balance in each cell). This reaction is thus not a major contributor of neutrons in the gold foils. Table XXVIII shows that if there is a self-shielding effect, the precision of these calculations is not tight enough to show it.

Table XXVIII. Results for Void Gold Foil Cells.

Reaction or Ratio	Result ^a	Difference from Nonvoid Result ^b (N σ)
$^{197}\text{Au}(n,2n)^{196}\text{Au}$	$7.70980\text{E}-08 \pm 3.43\%$	0.961
$^{197}\text{Au}(n,\gamma)^{198}\text{Au}$	$1.67486\text{E}-05 \pm 0.598\%$	1.53
Ratio	$4.60\text{E}-03 \pm 3.48\%$	1.13

^a Reaction rates are volume averages.

^b From Table XVI.

V. Summary and Conclusions

The IER-163 experiment on Comet achieved good results in the irradiation of foils and subsequent radiochemical analyses. The experiment produced R-values and activities for many important fission products, activation products, and actinides. The amount of ^{237}U , from $^{238}\text{U}(\gamma, 2n)$, and ^{239}Np in the uranium foils were also measured. There were six goals set forth in the CEDT-1 for this experiment.² All of these goals were achieved with the exception of measuring ^{115}Cd . Almost all the ^{115}Cd had decayed away by the time the irradiation foils reached LANL, and therefore it was decided not to run radiochemistry for it.

The MCNP model of IER-163 is a high-fidelity model but it lacks the exact locations of the copper reflector with respect to the active core; the exact assignment of Jemima plate materials to plate locations (plate dimensions are exact); and an exact description of the room and any other equipment within. Calculated k_{eff} values were consistent with what has been seen before for the HEU-MET-FAST-073, the fifth Zeus configuration: k_{eff} is too large when ENDF6 and ENDF7 neutron cross section are used and too small when ENDF5 cross sections are used.

The calculations showed that the uranium fission ratio $^{238}\text{U}(\text{n,f})/^{235}\text{U}(\text{n,f})$ was 12.6% too small when compared with measurements; this is also consistent with results previously obtained for Topsy and Flatop-25.

The ratio of plutonium to uranium fission, $^{239}\text{Pu}(\text{n,f})/^{235}\text{U}(\text{n,f})$, was too small by 10.1%.

The experimental fission ratios compared quite well with other experimental fission ratios from other critical experiments (Lady Godiva, and Topsy).

The iridium ratio $^{193}\text{Ir}(\text{n,n}')/^{191}\text{Ir}(\text{n,y})$ was 7.2% too large when computed using the T16_RC_2004 dosimetry library but 18.6% too large when computed using ENDF7 cross sections.

Gold was calculated very well. The gold ratios $^{197}\text{Au}(\text{n,2n})/^{197}\text{Au}(\text{n,y})$, $^{197}\text{Au}(\text{n,2n})/^{235}\text{U}(\text{n,f})$, and $^{197}\text{Au}(\text{n,y})/^{198}\text{U}$ were all within one standard deviation of the measured values.

If the computed ^{235}U fission rate were decreased by 10.1% and the computed ^{238}U fission rate were increased by 3.6% both uranium fission ratio and the plutonium fission ratios (with respect to ^{235}U , and ^{238}U fission) would be improved substantially compared to measurements. The $^{197}\text{Au}(\text{n,2n})/^{235}\text{U}(\text{n,f})$ ratio would also be improved, but the $^{197}\text{Au}(\text{n,y})/^{235}\text{U}(\text{n,f})$ ratio would be made worse compared to measurements.

There are several ways in which this experiment could have been improved. The most important is that the samples are recovered and shipped to radiochemistry labs sooner, so that their measurements are not activity limited. The time between EOB and start of counting at LANL approached ~10 days. LANL radiochemists typically prefer to have samples within ~2 days after EOB. Even though they were activity

limited for some isotopes by gamma spectroscopy, the separated sample results clearly demonstrate LANL's strong ability to perform low-level radiochemical analyses.

Finally, the counting room at NCERC could also use several improvements as well. There should be more and better calibrated HPGe detectors in order to do real quantitative gamma spectroscopy measurements on-site. There is also a need to match the source geometries to the calibrated sources. This will likely involve on-site swiping/de-contamination of samples upon retrieval from assemblies. The procedures at NCERC may need to be modified to provide this level of support.

In future experiments at NCERC, there will be the need to irradiate additional foils in different neutron energy spectra. One currently planned experiment, IER-136, is aimed at measuring fission chain yields for "peak yield" fission products on Flat-Top. The results that have been presented in this paper will be used to help shape the planning of these experiments.

REFERENCES

1. R. D. Mosteller, "The Unmoderated Zeus Experiment: A Cylindrical HEU Core Surrounded by a Copper Reflector," HEU-MET-FAST-073, in "International Handbook of Evaluated Criticality Safety Benchmark Experiments," NEA/NSC/DOC (95) 03, Nuclear Energy Agency, Organisation for Economic Co-operation and Development (Sep. 2009).
2. W. Myers, J. Bounds, and R. Sanchez, "IER 163: Reaction Rate and Fission-Product Yield Measurements with the Comet Assembly CEDT Phase-1 Detailed Plan," Los Alamos National Laboratory, LA-UR-11-05723, 2011.
3. J. Bounds, Internal Report and Communication, 2011.
4. K. R. Jackman, "KMESS: An Open-Source Software Package Using a Semi-empirical Mesh-Grid Method for the Modeling of Germanium Detector Efficiencies," Ph. D. Dissertation, The University of Texas at Austin, 2007.
5. J. Kleinberg, "Collected Radiochemical and Geochemical Procedures," Fifth Edition, Los Alamos National Laboratory, LA-1721, 1990.
6. T. R. England and B. F. Rider, "ENDF/349: Evaluation and Compilation of Fission Product Yields 1993," Los Alamos National Laboratory, LA-UR-94-3106, ENDF-349, 1993.
7. L. J. Koch and H.C. Paxton, "Fast Reactors," Annual Review of Nuclear Science, Vol. 9, 1959.
8. E. Sorensen, "Optional Zeus Spacer Disk Assy & Details," Los Alamos Laboratory Drawing No. 128Y-271100.
9. W. L. Myers, N-2, Los Alamos National Laboratory, personal communications, February 23, 2012.
10. W. L. Myers, N-2, Los Alamos National Laboratory, personal communications, March 5, 2012.
11. K. R. Jackman, T. A. Bredeweg, A. Schake, W. Oldham, J. Bounds, M. Attrep, and R. Rundberg, "Radiochemistry Results from the IER-163 Comet Irradiation," Los Alamos National Laboratory, LA-UR-12-20256.
12. J. A. Bounds, NEN-2, Los Alamos National Laboratory, email to J. A. Favorite and others, October 18, 2012.
13. R. S. Rundberg, C-NR, Los Alamos National Laboratory, personal communications, March 2012.

14. R. J. McConn, Jr., C. J. Gesh, R. T. Pagh, R. A. Rucker, R. G. Williams III, "Compendium of Material Composition Data for Radiation Transport Modeling, Revision 1," Pacific Northwest National Laboratory report PNNL-15870 Rev. 1, March 4, 2011.
15. "Dipotassium hexachloroiridate," http://www.chemicalbook.com/ChemicalProductProperty_EN_CB0457282.htm, accessed May 8, 2012.
16. A. C. Kahler, T-2, Los Alamos National Laboratory, "FlatTopTopsy.8Uf-5Uf-CE.xls," personal communications, May 1, 2012.
17. C. W. Wilkerson, "Zeus/Comet Irradiation," Los Alamos National Laboratory report, August 1, 2011.
18. C. W. Wilkerson, XTD-4, Los Alamos National Laboratory, personal communications, February 27, 2012.
19. R. G. Sanchez, N-2, Los Alamos National Laboratory, "Comet Startup and Acquisition of New Data," personal communication, March 6, 2012.
20. K. R. Jackman, C-NR, Los Alamos National Laboratory, personal communication, May 14, 2014.
21. M. B. Chadwick, S. Frankle, H. Trellue, P. Talou, T. Kawano, P. G. Young, R. E. MacFarlane, and C. W. Wilkerson, "Evaluated Iridium, Yttrium, and Thulium Cross Sections and Integral Validation Against Critical Assembly and Bethe Sphere Measurements," Nuclear Data Sheets, 108, 12, 2716-2741 (2007).
22. A. C. Kahler, T-2, Los Alamos National Laboratory, "193Ir(n,n')_tally.txt," personal communication, March 7, 2012.

ACKNOWLEDGMENTS

The authors would like to thank the following people for their support and commitment in this research project.

Robert Little, Tim Beller, Bill Haag, Eric Sorensen, Christopher Romero, George Brooks, Mike MacInnes, Don Dry, Michael Gallegos, Michael Cisneros, and Rowena Gibson.